2022 International Conference on Manipulation, Automation and Robotics at Small Scales (MARSS) | 978-1-6654-5973-0/22/$31.00 ©2022 IEEE | DOI: 10.1109/MARSS55884.2022.9870481

Eddy Current Damping of Magnetically Actuated Neurosurgical Instruments

Nancy Wu[1], Thomas Looi[2], Jim Drake[3], Eric Diller[4]

***Abstract*— Flexion based magnetically actuated minimally invasive neurosurgical tools tend to oscillate for an extended period of time due to the lack of avenues for energy dissipation. This study proposes eddy current damping as the mechanism for reducing the vibrations present for such magnetic tools. After determining the necessary damping coefficient (4.31×10^{-9} Ns m^{-1} for a settling time less than 0.5 s and 2.01×10^{-6} Ns m^{-1} for critical damping), a feasibility study was conducted by approximating the potential damping that could be generated. An experimental study was performed to validate these values and relationships determined by the approximations by measuring the oscillation of a 2 mm by 2 mm by 4 mm N52 Neodymium magnet attached to a nitinol beam. Six measurements were taken at gap sizes between the magnet and conductor of 0 μm, 100 μm, 200 μm, 300 μm, 400 μm, 500 μm, 750 μm, 1000 μm, 1500 μm, and 2000 μm with copper conductors of thicknesses 0.127 mm to 0.635 mm in 0.127 mm increments. It was shown that sufficient damping could be generated experimentally (the maximum damping documented is 1.24×10^{-6} Ns m^{-1}).**

I. INTRODUCTION

Progressively smaller and precise instruments are being developed for the benefit of society, but are often limited by the methods of actuation available. Recently, Lim et al. have developed magnetically actuated grippers to allow for increased versatility and precision of neuroendoscopic forceps [1], [2]. However, the fast response time of their tool and the inclusion of a flexion joint highlighted a problem with magnetic actuation: it has no way of removing energy from the system resulting in oscillation of the end effector. The study by Xu et al. suggests that longer latency of teleoperated tools is correlated to increased error, and a time of 300 ms was the maximum accepted time before a tool was considered cumbersome [3]. The current settling time of over 1000 ms necessitates a solution.

Damping is the one of the most well known method of removing energy from an oscillating system. Possible methods to provide damping torque include air friction damping, fluid friction damping, viscoelastic damping, active electromagnetic damping, and eddy current damping. Out of the listed, eddy current damping is the only mechanism that does not need a fixed reference goal position, scaling of complex components, or a lot of space. However, it is not known if eddy currents could provide sufficient force for magnetic surgical too stabilization. The purpose of this paper is to determine both theoretically and experimentally if the amount of force eddy current damping is capable of generating can adequately damp a neurosurgical instrument within 2% of its maximum amplitude within 300 ms. The metric by which eddy current damping will suggested as a suitable mechanism is determining if sufficient force can be generated for damping of a case study of the magnetically actuated flexion gripper (MAFG) fulfills criteria for the settle time and amplitude.

Thanks to the University of Toronto and the Hospital of Sick Children

[1]Nancy Wu is with the Institute of Biomedical Engineering, University of Toronto, ON M5S 3G9, Canada nj.wu@mail.utoronto.ca

[2]Thomas Looi is with the Hospital for Sick Children, PCIGITI, The Hospital for Sick Children, ON M5G 1X8, Canada thomas.looi@sickkids.ca

[2]James Drake is with the Hospital for Sick Children, Pediatric Neurosurgery, Department of Surgery, The Hospital for Sick Children, ON M5G 1X8, Canada james.drake@sickkids.ca

[4]Eric Diller is with the Department of Mechanical and Industrial Engineering, Microrobotics Lab, University of Toronto, ON M5S 3G8, Canada ediller@mie.utoronto.ca

II. BACKGROUND

Magnetic actuation was chosen for sugrical design in this study due to the simplicity of its implementation, the lack of space required, and the lack of specialized components required to utilize the mechanism. Tools developed with magnetic actuation can have high precision, directionality, and control complexity compared to tools with other actuation methods on the micro scale [4], [5]. However, tools with these qualities are often slow moving. In neuroendoscopy, both fast and precise movements are desired. This is because the brain is fragile, and shorter surgeries are beneficial to the patient.

As seen in 1he MAFG designed in [1] was developed for fast reaction time, capability of becoming tetherless, and two degrees of freedom. It features flexion joints which were chosen for their resistance to axial splitting/breakage and lack of friction typically present from joint components rubbing against each other. The latter is especially valuable given that the force of friction is significant at the micro scale and the generated force of magnetic actuation is weak in comparison to other small-scale actuation methods [6]. The MAFG consists of a "wrist" wire laser welded to a flexion joint connecting two titanium "fingers" (Fig.1), each 10 mm in length. The wrist bending joint is made from super elastic nitinol wire with a diameter of 0.125 mm and a length of 10 mm. The bending joint between the fingers is made out of 0.1 mm diameter nitinol wire that is 3 mm in length. A total of three magnets are laser welded to the gripper. The first magnet (4 mm by 2 mm by 2 mm) is welded to the wrist wire. The second and third magnet (3 mm by 1 mm by 1 mm) are the magnets welded to the left and right titanium finger respectively. The bending of the wrist and adduction or abduction of the fingers are caused by deflection of the magnets in response to an applied uniform directional magnetic field $B_{\parallel}$ Fig.1-B. The desired flexion angles were 90° in each direction for the wrist and 10° inwards for the fingers relative to their positions with no field applied.

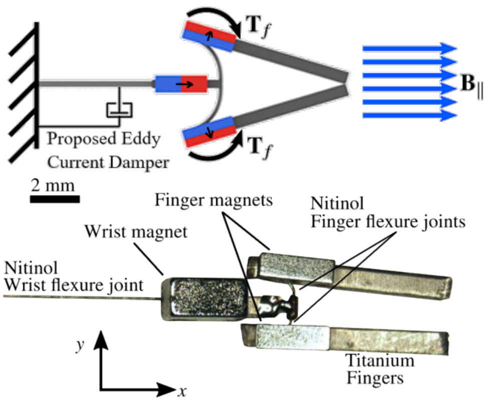

Fig. 1. Explanatory diagram of grippers adapted from [1]. Above, blue arrows show the direction of the magnetic field. Black arrows on the red and blue magnets show magnetization direction and torque direction in response to the magnetic field. Below the MAFG created by Lim et al. [1]

Unfortunately, the MAFG suffers from vibrations and aside from the friction provided by the surrounding fluid (air or cerebrospinal fluid), there is very little stopping force. This makes the kinetic energy added to the system from inducing movement of the MAFG difficult to dissipate 1. If the amount of time the tool takes to settle is cumbersome to the surgeon or extends the surgery long enough to be detrimental to the patient, the tool is not useful [1].

III. THEORETICAL EDDY CURRENT DAMPING ESTIMATES

To determine the feasibility of using eddy current as a source of damping, how much damping is already present in the system (the inherent damping) needs to be known. This parameter was calculated using the gripper movement data provided by [1]. To record this data, Lim et al. used a Net GmbH FO124TC firewire camera, with the resolution of 640 by 480 pixels and a frame rate of 60 fps. The resulting data was imported and processed with MATLAB. It was then fitted to the solution of a damped spring equation (1).

$$\theta(t) = A_0 e^{\frac{C}{2j}t} \cos(\omega_d t + \phi), \quad (1)$$

For inertia j, damping coefficient C, spring constant k, damped frequency ω_d, angular position θ, phase offset ϕ, and initial oscillation amplitude A_0.

The fast Fourier transform yielded the oscillation frequency of the gripper in air ($f_o = 9.50$ Hz). This frequency was used as the natural frequency to calculate the inertia of the gripper (j = 4.26×10^{-10} kg m^2). Using this inertia, the innate damping was calculated to be 4.31×10^{-9} Ns m^{-1}. After finding the inherent damping, the total required damping needs to be determined. The critical damping value (C_c = 2.01×10^{-6} Ns m^{-1}) corresponds to the fastest settling time. While achieving critical damping is ideal, as long as the tool achieves a 2% settling time of less than 300 ms, a lower damping value is acceptable. For the MAFG, this value was determined to be 1.11×10^{-8} Ns m^{-1}. Subtracting the inherent damping value from this constant, the final target value was derived to be 6.79×10^{-9} Ns m^{-1}.

To determine the amount of damping that can theoretically be generated from a system on a similar scale, past literature was consulted. Four works were chosen to corroborate the estimation. The literature selected were works from four authors: Eddy current of a magnet moving through a pipe by Kenneth D. Hahn, Magnet fall inside a conductive pipe: motion and the role of the pipe wall thickness by Guillermo Donoso, Modeling and Analysis of Eddy-Current Damping Effect in Horizontal Motions for a High-Precision Magnetic Navigation Platform by Moein Mehrtash, and Improved concept and model of eddy current damper by Henry A. Sodano. Aside from relevance, a short explanation on why each paper was chosen will be expressed. The key equations were identified and necessary adaptations were made before being solved in MATLAB. The parameters were chosen to resemble the surgical tool in the setup as well the parameters used for the experimental validation. The magnetic material will be assumed to be a 2 mm by 2 mm by 4 mm N52 Neodymium magnet with a remanence of 1.48 T and an approximate mass of 1.12×10^{-4} kg. The thickness of the copper will be 0.02". In the case that there is no infinite plate/pipe conductor assumption, the dimensions of the copper will be assumed to be a 3 mm by 10 mm or a pipe of length 10 mm and a conductivity of 5.96×10^7 S/m. The distance from the magnet to the copper will be 0.25 mm.

A. *Conductive Tube Model*

1) Infinite Conductive Tube Model: The first work examined is by Hahn et al.. Their method was chosen because their model was based on the most fundamental and simple model– a magnet moving through a conductive tube [7]. Notable differences between their model and this study are that their magnet is fully surrounded, untethered, cylindrical. Their experiment was conducted in an axially symmetric system. Some assumptions about and approximations to the system under investigation were made in order to conform to the assumptions of Hahn et al.'s work. These are as follows:

- Due to small angle deflections, the arc caused by pivoting about the oscillator can be neglected. Thus this experiment can be modeled as a magnet moving along a single axis.
- The damper can be modeled as a conductive tube surrounding the magnet, and small gaps along the length of the pipe do not affect the results.
- A cylindrical magnet produces the same magnitude of eddy currents as a rectangular prism provided the volume and the average distance between the surface of the magnet and the conductor is the same.
- A permanent magnet can be approximated by a magnetic dipole positioned at the center of the permanent magnet. This allows us to represent the field generated

by a magnetic moment (m_B) at each point in the tube in cylindrical coordinates (r, x, θ), by

$$B_r(x) = 3\frac{\mu_0 m_B}{4\pi}\frac{rx}{(r^2+x^2)^{5/2}}, \tag{2}$$

where (0,0,0) is the center of the dipole.

- The pipe is infinitely long.
- The magnetic flux vectors pointing to the ends of the pipe can be ignored.

Hahn's process can be summarized as (3):

$$F_{damping} = \frac{9\mu_0^2\mu_B^2}{8\pi}\sigma v\int_{bottom}^{top}\int_{R_1}^{R_0}\frac{r^3x^2}{(r^2+x^2)^5}drdx. \tag{3}$$

With this equation, the force from the eddy currents can be approximated. Then, using the relationship ($F = -Cv$) the magnitude of the damping coefficient is determined [7]. Using this process the damping coefficient C was found to be 0.11 Ns m^{-1}. This exceeds the target values (critical damping and damping for a settling time within 300 ms).

According to 3 the variables that have the most effect on the damping include the magnet to conductor distance(r_0), the magnetic volume (V_m), and the conductor thickness($r_0 - r_1$ or δ). The relationship between damping coefficient and magnetic volume (assuming constant remenance) can be expressed as $V_m \propto m_b \propto \sqrt{C}$. Fig.2-A illustrates how the thickness, pipe length, and gap size/inner radius affect the damping coefficient. As expected, the most damping results from the combination of the smallest gap size, greatest conductor length, and greatest thickness. Between the three variables, changing the thickness appears to have the smallest effect on damping.

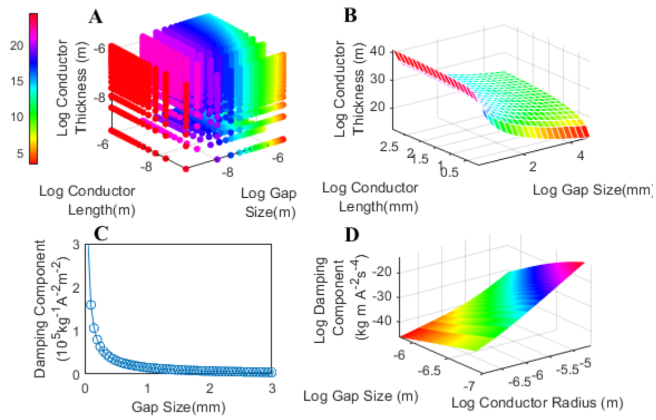

Fig. 2. A. The log-log-log graphs resulting from varying pipe length (100 μm to 5000 μm), thickness (100 μm to 3000 μm), and gap size (100 μm to 3000 μm) accordance with (3) for Hahn et al. The color map represents the log value of the damping coefficient component. B. The linear-log-log graphs resulting from varying pipe length (100 μm to 5000 μm) and gap size (100 μm to 3000 μm) in accordance with (4) for Donoso et al. C. The graph representation of gap size with the damping coefficient from Mehrtash's equations. D.The log-log-log graph resulting from graphing the damping coefficeint in relation to conductor size of Sodano et al.'s equations (6).

2) *Infinite Tube Model with Small Thickness:* The geometry of Donoso's model, the basic concept, and the processes were all highly similar to that of Hahn et al. Aside from the additioanl assumption of the thickness being far greater than the magnet to conductor distance, the same assumptions made in III-A.1 were made for Donoso's model.

Donoso's estimation is summarized as follows:

$$F_{damping} = 36\pi m_B^2\delta\sigma v\int_{-\infty}^{\infty}\frac{x^2r^3}{(r^2+x^2)^5}dx, \tag{4}$$

Where δ represents conductor thickness. Recalling the relationship $F = -Cv$, the damping coefficient is found to be 2.75×10^{-5}Ns m^{-1}.

In the equation derived by Donoso et al. (see (4)), the relationships between the damping coefficient and thickness or the amount of magnetic material (assuming the a constant material) are as follows: $V_m \propto m_b \propto \sqrt{C}$ and $\delta \propto C$. The graphical representation of gap distance embedded in the integral of (4) can be seen in Fig.2-B.

B. Conductive Sheet Model

1) *Infinite Conductive Sheet Model:* Mehrtash et al.'s model was selected due to the geometric simplicity and resemblance to the model for the study. The setup in this work consists of a pseudo-magnetic microrobot that was actuated over a sheet of conductive material. The differences between his study and the situation outlined in this paper are predominantly the source of magnetic field (a electromagnet and a permanent magnet) and the size of the conductor. For the equations derived by Mehrtash et al. the following assumptions were made:

- The model for the MAFG, reduced to a magnet flanked by two conductor planes, provides exactly double the amount of damping of a magnet over a single plate.
- The conductive plates are thin and infinitely long (such that all effects are uniform).
- Permanent magnets (and electromagnets) supplying the magnetic field can be modeled as current-carrying loops with alternating currents.

Because no electromagnet was used in the setup of this experimental study, the components of the equation that represent the effects of the electromagnet must be removed. After the adjustments the equation for the damping force can be expressed as

$$F_{damping} = \mu_0^2 v\sigma\delta I_1^2 r_{loop}^2\int_0^{\infty} gJ_1^2(gr_{loop})e^{-2gd_1}dg. \tag{5}$$

In this equation, $g = \sqrt{r_{loop}^2+\phi^2}$ and J_1 is a first order Bessel function [8]. Combined with $F = -Cv$, Mehrtash et al.'s method results in the value 2.02×10^{-4} Ns m^{-1}.

The relationships of the independent variables to the damping coefficient include a direct proportion to magnitude of the current or strength of the magnetic moment ($I_1 \propto m_B$), and consequently the magnetic volume ($\sqrt{C} \propto m_B \propto V_m$). Thickness is directly proportional to the damping coefficient ($C \propto \delta$) while d_1, the magnet to conductor distance, has a complex relationship and is embedded into the exponential.

2) Finite Sheet Models: The model derived by Sodano et al. was chosen for its high degree of similarity to the model of this study [9]. The main difference is the scale and that the distance between the conductor and magnets are not constant over the course of the measurement.

For this method, the following assumptions are made:

- The surface charges can be ignored.
- The damping force is a constant value corresponding to the mean distance between the magnet and beam.
- A circular conductor would generate the same quantity of eddy currents in comparison to a rectangular conductor with the same surface area.
- The frame of reference can be transformed from the frame of the magnet to the frame of the conductor

Unlike the previous studies, Sodano et al. models the fields of the permanent magnet as a hollow cylinder.The resultant flux density (B_y) is then integrated into the Lorentz force equation. This resulting in the equation:

$$F = -2\pi\sigma\delta v \int_0^{r_c} y B_y^2(y, I_g) dy \quad (6)$$

Where δ is thickness, v is vertical velocity, r_c is the equivalent radius of the conductor that preserves its surface area, σ is conductivity, I_g is the distance between the conducting sheet and the bottom of the magnet. B_y is the horizontal component of the magnetic field of the permanent magnet and r_m is the radius of the circular magnet. From this method, the damping coefficient comes out to be: 8.1×10^{-3}Ns m^{-1}.

Equation (6) identifies a direct relationship between the damping coefficient and thickness ($C \propto \delta$). The magnetic dipole and thus the magnetic material is proportional to the damping coefficient ($\sqrt{C} \propto m_B$). The complex approximetely exponential relationship between conductor surface area or gap size and the damping coefficient is visualized in Fig.2-D. The relationships appears approximately exponential and the largest coefficients resulted from the smallest gap size and largest conductor radius.

IV. EXPERIMENTAL EDDY CURRENT DAMPING

The purpose of the setup is to position the magnet and copper relative to each other, provide the initial actuation to start the movement of the oscillator (along the z-direction/in and out of the page relative to Fig.3), the oscillators movement response with respect to different thicknesses of and proximity to the sheet conductors. Note that the oscillator does not swing from a pivot point, but rather oscillates due to slightly bending of the nitinol wire.

A. Damping Setup Preparation and Measurement Process

The measurements were taken using ScanCONTROL Configuration Tools 6.4 at 140 Hz to interface with the ScanControl 2900-10BL laser scanner. The data was then processed and fitted with MATLAB.

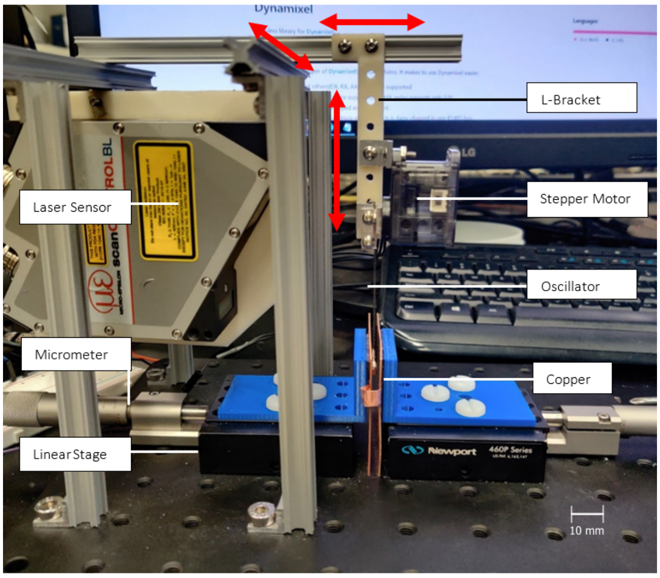

Fig. 3. A labeled depiction of the final setup used for experimentation. The red lines show how the relative distance between the copper plating, laser sensor, and the oscillator can be changed [1].

To observe the behavior of the damping coefficient at different volumes/thicknesses of conductor and gap distances between the conductor and magnet, 6 samples were taken of every permutation of the following: gap distances of 0 μm, 100 μm, 200 μm, 300 μm, 400 μm, 500 μm, 750 μm, 1000 μm, 1500 μm, and 2000 μm with copper of thickness 0.127 mm to 0.635 mm in 0.127 mm increments. To observe the effect of different quantities of magnetic material, the movement responses of oscillators with 1, 2, and 3 magnets (2 mm by 2mm by 4 mm, N52 Neodymium magnets) were tested at a gap distance of 750 μm and between two copper plates of 0.508 mm thickness. As all measured curves are underdamped, the equation the data was fitted to an decaying cosine exponential in MATLAB with the addition of free parameters for vertical (for curves imperfectly centered about 0) and horizontal shifts (time lag).

B. Damping Coefficient Experiment Results and Discussion

The experiment endeavors to confirm the hypothesis that eddy current damping can generate forces that exceed the estimated damping constant target values and confirm the theoretical relationships of the variables of interest (gap size, conductor size, magnetic volume, and thickness) to the damping coefficient on the micro scale. The utmost care was taken to ensure it resembled the studied situation as closely as possible.

1) Eddy Current Damping Coefficient Reactions to Changes in Magnetic Material: The effect of changing magnetic strength is depicted in Fig.4. It can be observed that the without the presence of copper (and consequently no eddy current damping) the differences in mean damping coefficient between the two measurements with the same quantity of magnets were less 2×10^{-8} Ns m^{-1}. Additionally, all damping coefficients fell within 2×10^{-7} Ns m $^{-1}$ for

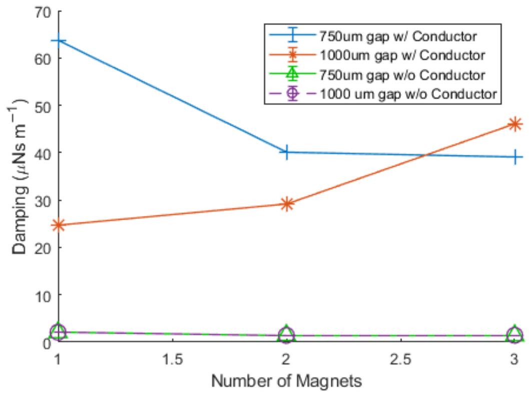

Fig. 4. Depicted are four data sets taken of the oscillator's position after a pseudo delta impulse generated by the actuation of a servo motor. Twelve total data sets were taken corresponding to each permutation of magnetic material volume (2 mm by 2 mm by 4 mm N52 magnets) and gap size, and 0.020" copper conductor presence. Each coefficient has been normalized by the inertia of their corresponding oscillator.

all magnet quantities. This suggests the sole contributor to the changes in damping coefficient is caused by changes in degree of eddy current damping other sources of error make little difference to measurements when properly normalized by their inertia. It should also be noted that at both distances, the damping coefficients of the control data were on the order of 10^{-7} Ns m^{-1}.

The change in magnetic material did not affect the damping in the predicted manner. Every model suggested that an increase in magnetic material would correspond to an increase in damping. While the data collected behaved as expected at a gap size of 1000 μm, the data did not behave as expected when a gap size of 750 μm was used. The 1000 μm set is observed to have an increasing damping coefficient with an increase in magnetic materials while 750 μm appears stagnant. Although the closer distance should have resulted in stronger eddy current damping due to proximity, the change in damping coefficient between the different quantities of magnetic material was minimal.

A possible reason for the difference in behaviors between the 750 μm curve and 1000 μm curve is that the magnet can no longer be approximated by a dipole at the closer distance, as the local fields of the three magnets may be interfering destructively causing a different geometry of magnetic field.

2) Eddy Current Damping Coefficient Reactions to Changes in Distance Between the Magnet and the Conductor: Fig.5 explores the relationship between the damping coefficient and the gap distance (between the magnet and the conductor). For gap distances of 100 μm or larger, the relationship between the damping coefficient and air gap distance (between the magnet and the conductor) follows an approximately monotonic decay as predicted by Hahn et al. The relationships between the coefficient and the parameters, however, remain inconclusive. The damping coefficients of the 0.381 mm conductor and the 0.508 mm conductor are suspiciously close in values at all distances. At distances less than 100 μm, the damping coefficient varies wildly in

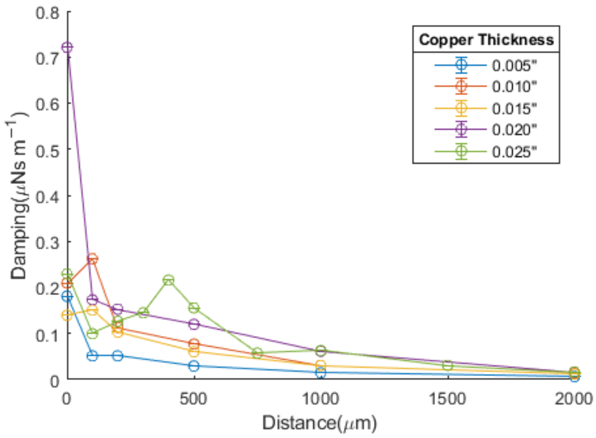

Fig. 5. A visualization of the relationship between the damping coefficient and the gap distance in μm repeated with a variety of thicknesses of copper. 6 measurements/samples were taken at each permutation of gap distance and conductor thickness. The minimum distance, denoted 0 μm, is the closest point at which the oscillator appeared to swing freely between the conductor with no obvious sign of impact. The oscillator used was a 75 mm nitinol beam with a 2 mm by 2 mm by 4 mm magnet.

magnitude. This is likely due to the unpredictable, inconsistent effects of start point calibration, friction, and impact damping. This is supported by the comparatively large variances of the data points at 0 μm. The data set however, can establish the efficacy of eddy current damping from the significant difference in damping coefficient magnitudes when comparing the data sets with and without a conductor.

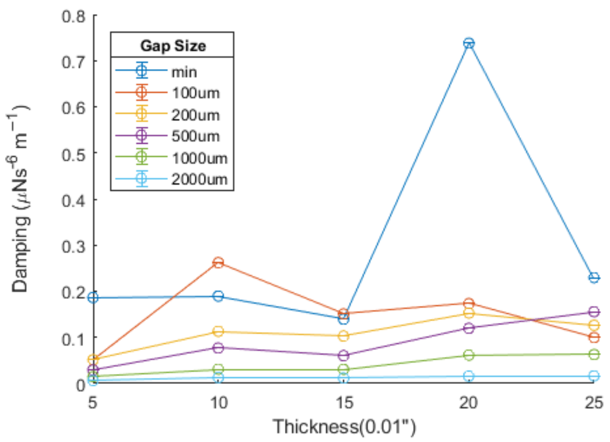

Fig. 6. A visualization of the relationship between the damping coefficient and the thicknesses of the conductor. The oscillator used was a 75 mm nitinol beam with a 2 mm by 2 mm by 4 mm magnet. This graph uses the same data set as the one used to plot Fig.(5). The data is plotted with respect to thickness of conductor used. To ensure independence of curve shape from gap size, the datasets shown are separated by the conductor and magnetic material gap distance.

3) Eddy Current Damping Coefficient Responses to Changes in Conductor Thickness: Fig.6 depicts the damping coefficient in relation to the thickness of the conductor. Referring to Section III, a proportional relationship between thickness and the damping coefficient was expected. With the exception of a few outliers, the general trend between thickness and damping coefficient in Fig.6 was consistent with this expected behavior.

V. CONCLUSIONS

While MIS has been comfortably established for most parts of the body, its benefits can be further enhanced. The qualities of being minimally intrusive and precise are the biggest advantages of MIS and areas like the brain would benefit from further improvement.

Magnetically actuated neurosurgical tools, such as those developed by Andrew Lim and Cameron Forbrigger, are examples of such attempts [1] [2]. Magnetic actuation contains many benefits such as a wireless power source and simplicity. Unfortunately, magnetic actuation is not very strong and has often has difficulty stopping sharp movement.

From this study, it has been demonstrated experimentally and theoretically that the force generated through eddy current damping can generate a sufficiently strong effect to stabilize neurosurgical instruments on the micro scale. This suggets that there is a potential for a new breed of microsurgical instruments that are less complex, and thus easier to scale down and safer due to lower chance of failure. Additionaly, instruments designed with this actuation mechanism has potential to be tetherless. This research can also be applied to any tools and robotics of a similar scale or space constraint as long as there are no factors interfering with the magnetic actuation mechanism.

This study did not, however, provide a demonstration or achieve the objective of concretely identifying and establishing the relationships between eddy current damping and its variables due to the high degree of uncertainty. To properly establish the relationships, consistency, repeatability, and precision needs further development. Therefore, one future direction would be a repeat of this study using a setup with significantly higher precision and repeatability to properly establish variable relationships on the micro level. The extensive use of robotics, such as during manufacturing, initial actuation, and positioning would make the position, angle, and properties of the oscillator more consistent. The behaviour could then be more accurately explained through a dynamic simulation, an electromagnetic field analysis, and an structural vibration analysis. It is also recommended that this study could also be performed in vitro to provide a more representitive gauge of the effectiveness. A practical future direction would be fabrication of eddy current dampers to further ascertian the effectiveness of eddy current damping.

ACKNOWLEDGMENT

We thank the other members of the friends and family, members of the Microrobotics Lab, and members PCIGITI for support.

REFERENCES

[1] A. W. Lim, *Wireless Magnetically-Actuated Dexterous Forceps Instruments for Neuroendoscopy*, Dept. Mech. and Ind Engineering. Univ, Tor, Toronto, Canada, 2019.

[2] O. O. C. Forbrigger, A. Lim, "Cable-less, magnetically-driven forceps for minimally invasive surgery," *IEEE Robotics and Automation Letters*, 2019.

[3] K. Y. S. Xu, M. Perez, "Determination of the latency effects on surgical performance and the acceptable latency level in telesurgery using the dv-trainer simulator," *Springer Science*, vol. 28, pp. 2569-2576, 2013.

[4] X.-Z. Chen, B. Jang, D. Ahmed, C. Hu, C. Marco, M. Hoop, F. Mushtaq, B. Nelson, and S. Pane, "Small-scale machines driven by external power sources," *Advanced Materials*, vol. 30, pp. 1 705 061 1–22 ,, 2018.

[5] F. Leong, N. Garbin, C. Natali, A. Mohammadi, D. Thiruchelvam, D. Oetomo, and P. Valdastri, "Magnetic surgical instruments for robotic abdominal surgery," *IEEE Reviews in Biomedical Engineering*, vol. 9, pp. 66–78,, 2016.

[6] M. M. Jake J. Abbott, E. Diller, and A. J. Petruska, *Annual Review of Control, Robotics, and Autonomous Systems*, vol. 3, no. 1, p. 57–90, 2020.

[7] A. B. K. D. Hahn, E. M. Johnson, "Eddy current of a magnet moving through a pipe," *American Journal of Physics Teachers*, vol. 66, pp. 1066-1075, 1998.

[8] M. B. K. M. Mehrtash, "Modeling and analysis of eddy-current damping effect in horizontal motions for a high-precision magnetic navigation platform," *IEEE Transactions on Magnetic*, vol. 49. no. 8. 4801-4810, 2013.

[9] D. I. H. Sodano, J.Bae, "Improved concept and model of eddy current damper," *Trans. ASME*, vol. 127, no.3, pp.294-302, 2006.